npg

ORIGINAL ARTICLE

Interfacial engineering of epoxy/carbon nanotubes using reactive glue for effective reinforcement of the composite

Tsuyohiko Fujigaya[1,2], Yusuke Saegusa[1], Shogo Momota[3], Nobuhide Uda[3] and Naotoshi Nakashima[1,2]

We describe a novel strategy for reinforcing an epoxy resin using carbon nanotubes (CNTs), in which polybenzimidazole (PBI) was used as the glue to enable effective adhesion between the epoxy matrix and the CNT surface. Because PBI strongly interacts with the surfaces of the CNTs and reacts with epoxy matrices to form covalent bonds, the PBI-wrapped CNTs are a promising novel epoxy-CNT hybrid. The PBI-wrapped CNTs (CNT/PBI) exhibited an effective reinforcement of the epoxy resin hybrid, resulting in a higher tensile strength and Young's modulus (that is, +28.1% and +8.8%, respectively) compared with those of the hybrid using oxidized CNTs in place of PBI-wrapped CNTs (+18.6% and − 4.8% reinforcement for tensile strength and Young's modulus, respectively). Scanning electron microscopy measurements of the fracture surfaces of the CNT/PBI-epoxy hybrid revealed that only very short CNTs were observed for the CNT/PBI-epoxy hybrid due to effective load transfer resulting from the formation of covalent bonds between the PBI on the CNTs and the epoxy resin, which is in contrast to that observed for oxidized CNT-epoxy, which exhibited long CNTs in the fracture surfaces owing to slippage at the interfaces.

INTRODUCTION

Carbon fiber reinforced plastics (CFRPs), which are typically composed of carbon fiber (CF) and an epoxy resin, have attracted much attention as alternatives to metal-based materials owing to their remarkable mechanical properties, as well as being lightweight.[1,2] One of the most successful examples of a CFRP is its use as structural materials in aircraft, in which the total weight of the aircraft was reduced by 20% owing to the replacement of ~ 50% of the aluminum-based material with a CFRP-based material. This reduced weight substantially decreased the fuel consumption as well as CO_2 emissions. This success motivated industrial research to further improve their material properties while maintaining their light weight. A promising strategy involves the replacement of CF with stronger materials. Therefore, carbon nanotubes (CNTs) with a higher Young's modulus of 270–950 GPa and tensile strength of 11–63 GPa[3] than those of CF (typically, 200–700 GPa and 3–7 GPa for Young's modulus and tensile strength, respectively) have emerged as promising alternatives.

However, unlike CF, CNTs form strong bundle structures that hinder homogeneous mixing with an epoxy matrix.[4] When the dispersion of CNTs in epoxy matrices is poor, the CNT bundles tend to induce a stress concentration, which hampers the effective reinforcement of the composites.[5] In addition, the interfacial adhesion between the CNTs and the matrix is very weak, resulting in insufficient load transfer to the CNTs in the composites. Therefore,

the primary requirement for effective reinforcement is homogeneous dispersion of the CNTs in the epoxy matrices. Several types of strategies for dispersing CNTs into epoxy matrices have been investigated to improve the wettability with an epoxy matrix.[6–16] The studies include (i) the dispersion of CNTs using surfactants, such as sodium dodecyl sulfate and Triton X, before mixing with an epoxy resin,[4,17] (ii) the surface oxidation of CNTs,[18] (iii) the surface modification of the CNTs with either functional groups or polymers based on covalent bonds and (iv) surface wrapping with a polymer-based non-covalent functionalization.[19] The second requirement for effective reinforcement is effective load transfer between the CNTs and the epoxy matrix,[20] and covalent bonding between surface functional groups on the CNTs and the epoxy resin has been proposed.[21–24] However, the introduction of a covalent bond typically induces damage to the surface of the CNTs, which decreases their mechanical toughness.[25] Therefore, a novel strategy for achieving effective load transfer along with homogeneous dispersion of the CNTs into the epoxy resin while maintaining the intrinsic structure of the CNTs is needed.

In this study, we explored a novel strategy that involves a specific polymer with a strong affinity for CNT surfaces as well as reactivity with the epoxy monomer being used as reactive 'glue' between the CNTs and the epoxy resin. Polybenzimidazole (PBI) was selected as the polymer, as PBI has a strong affinity for the surfaces of CNTs,

[1]Department of Applied Chemistry, Graduate School of Engineering, Kyushu University, Fukuoka, Japan; [2]International Institute for Carbon-Neutral Energy Research (WPI-I2CNER), Kyushu University, Fukuoka, Japan and [3]Department of Aeronautics and Astronautics, Graduate School of Engineering, Kyushu University, Fukuoka, Japan
Correspondence: Dr T Fujigaya or Professor N Nakashima, Department of Applied Chemistry, Graduate School of Engineering, Kyushu University, 744 Motooka, Nishi-ku, Fukuoka 819-0395, Japan.
E-mail: fujigaya-tcm@mail.cstm.kyushu-u.ac.jp or nakashima-tcm@mail.cstm.kyushu-u.ac.jp

which provides homogeneous CNT dispersion on the basis of a stiff nanometer-thick coating (1–2 nm) on the CNTs,[26–29] and the polymer has an imidazole moiety in the main chain, which can be used as a reactive site with the epoxy group.[30–33] Yang *et al.* reported a similar concept, reinforcing the epoxy-CNT composite using a pyrene derivative carrying an epoxy unit, in which the pyrene group interacts with the surface of the CNTs and the epoxy unit reacts with the epoxy matrix.[34,35] However, CNT aggregation was observed for composites with only a 0.3 wt% loading of CNTs, which was most likely owing to insufficient coating of the CNTs with the pyrene derivative. In general, non-covalent functionalization of CNTs with small molecules is an equilibrium process and requires an excess amount of solubilizer in the bulk solution.[36] Therefore, these dispersant molecules are easily detached from the CNT surfaces resulting in aggregation when the third additive (that is, epoxy resin in this case) is added. In contrast, non-covalent modification of CNTs using polymeric dispersants is sufficiently strong, which leads to the formation of a homogeneous CNT-epoxy composite.

EXPERIMENTAL PROCEDURE

Materials

Multi-walled carbon nanotubes (purity > 95%, diameter 40–90 nm), which were purchased from Hodogaya Chemical (Tokyo, Japan), were used as the CNTs. The epoxy resin (diglycidyl ether of bisphenol A, JER 807) and curing agent (aromatic amine, JER-CURE W) were obtained from Mitsubishi Chemical (Tokyo, Japan). DMAc (*N,N*-dimethylacetamide), phosphoric acid and sodium hydroxide were purchased from Kishida Chemical (Osaka, Japan), Nacalai Tesque (Kyoto, Japan) and Wako Pure Chemical (Osaka, Japan),
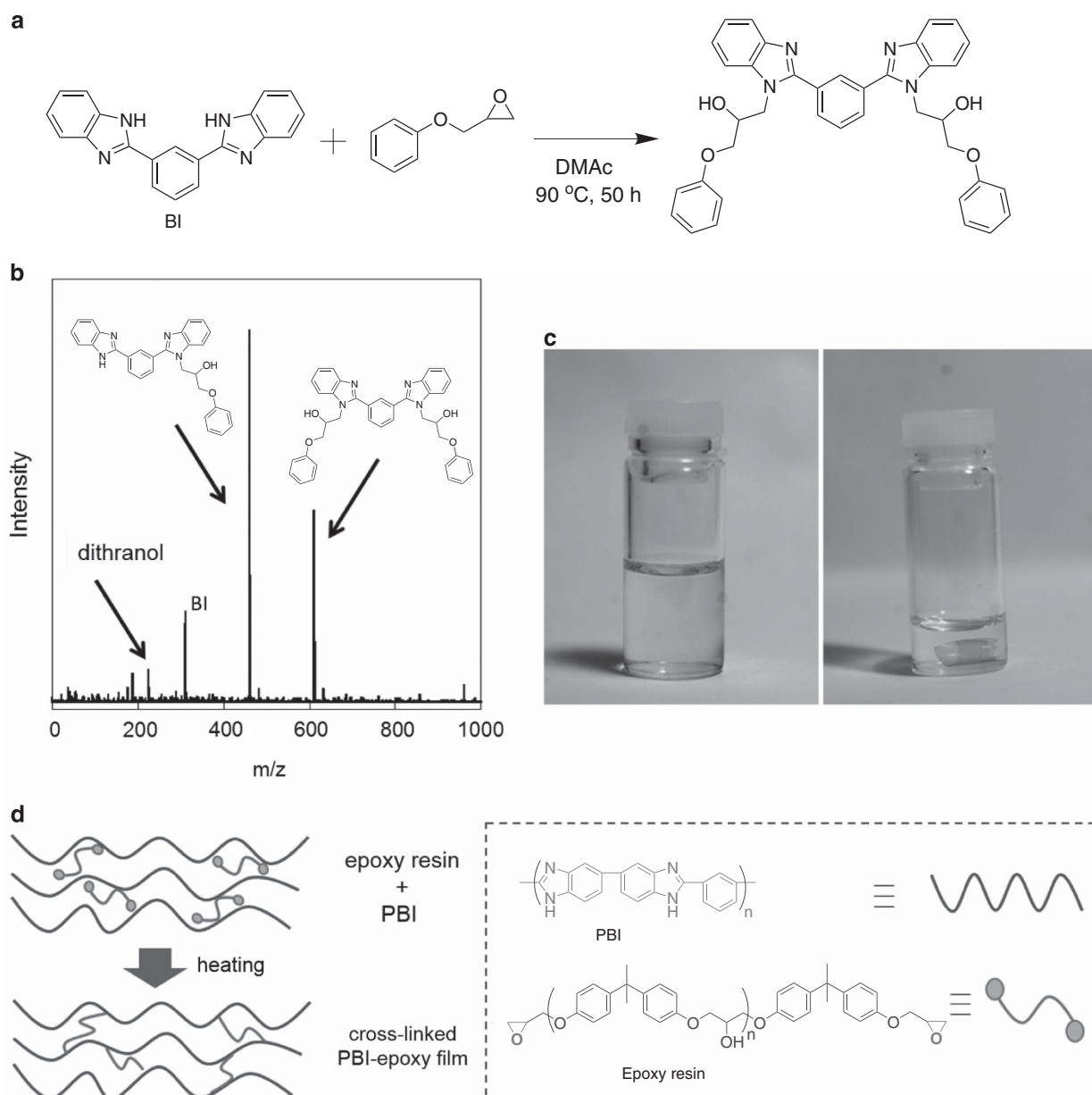

Figure 1 (a) Scheme of the model reaction between BI and glycidyl phenyl ether. (b) MALDI-TOF MS spectrum of the product of the model reaction. (c) Photos of the PBI film without (left) and with (right) the epoxy dissolved in DMAc by heating. (d) Schematic illustration of cross-linking of the PBI film containing epoxy resin by heating. BI, 2,2'-*m*-phenylenebisbenzimidazole; DMAc, *N,N*-dimethylacetamide; PBI, polybenzimidazole. A full color version of this figure is available at *Polymer Journal* online.

respectively. 1,2-Phenylenediamine and DMF (N,N-dimethylformamide) were purchased from Sigma-Aldrich Japan (Tokyo, Japan). Isophthalic acid and glycidyl phenyl ether were purchased from TCI (Tokyo, Japan). All of the chemicals were used as received. PBI was obtained from Sato Light Industrial (Tsu, Mie, Japan).

Characterization

The ^{1}H NMR and FTIR spectra were measured using an AV 300 M spectrometer (Bruker Biospin, Yokohama, Japan) and a Spectrum 65 FTIR (PerkinElmer Japan, Yokohama, Japan) spectrophotometer equipped with an ATR apparatus with a resolution of $4 \, cm^{-1}$, respectively. The MALDI-TOF mass (MS) spectrograph was obtained using an Autoflex (Bruker Daltonics, Yokohama, Kanagawa, Japan). The fracture surfaces of the composites were observed using scanning electron microscopy (SU9000, Hitachi High-Tech, Tokyo, Japan) with an accelerating voltage of 10 kV. For the tensile test, the composites were cut into rectangular specimens that were 60 mm × 8 mm × 1-mm. The extension rate and gauge length were $1 \, mm \, min^{-1}$ and 20 mm, respectively. The tests were performed using an Autograph AG 5000 (Shimadzu, Kyoto, Japan) with a 2 kN load cell.

Preparation of a MWNT/PBI

To PBI (4.0 mg) dissolved in DMAc (20 ml), the CNTs (20 mg) were added and sonicated for 3 h using a bath-type sonicator (BRANSON 5510). Then, the mixture was filtered and washed with DMAc to remove any unbound PBI. The obtained solid (CNT/PBI) was dried in vacuum at 80 °C for 24 h.[27]

Plasma functionalization of CNTs

The CNTs were oxidized using a low-pressure RF plasma system (CUTE-MP/R, FEMTO Science) at 50 kHz and a power of 200 W under an oxygen flow at $10 \, s.c.c.m. \, min^{-1}$ at 0.48 Torr for 60 min.

Synthesis of 2,2'-m-phenylenebisbenzimidazole (BI)

Isophthalic acid (0.166 g, 1.00 mmol) was stirred with 1,2-phenylenediamine (0.234 g, 2.20 mmol) in phosphoric acid (10 ml) at ~200 °C for 5 h. The colored melt product was poured into 200 ml of vigorously stirred cold water.

After cooling, the generated precipitate was collected by filtration and dispersed in a 10% aqueous sodium carbonate solution (100 ml). Then, the resulting solid was filtered and dried in vacuum at 60 °C in the presence of V_2O_5 to afford a white powder (0.243 g, 78.4%).[37]

^{1}H NMR (300 MHz, DMSO-d_6): δ/p.p.m. 13.30 (s, 2H), 9.07 (t, $J = 3.0$ Hz, 1H), 8.28 (dd, $J = 3.0$, 9.0 Hz, 2H), 7.75 (t, $J = 9.0$ Hz, 1H), 7.65 (br, 4H), 7.28-7.22 (m, 4H). ^{13}C NMR (75 MHz, DMSO-d_6): δ/p.p.m. 150.7, 130.9, 129.6, 127.5, 124.6, 122.2. FTIR (ATR): 3063, 1439, 1281, 1232, 802, 727 cm^{-1}. MALDI-TOF MS (Matrix: dithranol): m/z for $C_{20}H_{14}N_4$, $[M+H]^+$ calculated 311.12, found 311.17.

Reaction of BI with glycidyl phenyl ether

BI (2,2'-m-phenylenebisbenzimidazole; 0.31 g, 1.0 mmol), which was dissolved in N,N-dimethylformamide (5 ml), was added to glycidyl phenyl ether (0.30 g, 2.0 mmol), and the mixture was stirred at 90 °C for 50 h under a nitrogen atmosphere. The mixture was poured into water to produce a precipitate, which was collected by filtration and purified by silica gel chromatography using ethyl acetate as the eluent. The obtained solid was dried at 80 °C for 24 h to yield an orange solid (0.22 g, yield 36%).[38] IR (ATR): $\nu = 1587$ ($\nu_{C=N}$), 1440 (δ_{C-N}), 1243 (ν_{C-O}): MALDI-TOF MS m/z for $C_{38}H_{34}N_4O_4$, $[M+H]^+$; calculated 611.26, found 611.49; m/z for $C_{24}H_{24}N_4O_2$, $[M+H]^+$; calculated 461.19, found 461.24.

Fabrication of epoxy-based cross-linked PBI membrane

PBI (100 mg), which was dissolved in DMAc (2.0 ml), was added to an epoxy resin (20 mg) under mechanical stirring. Then, the mixture was cast on a glass dish and dried at 80 °C for 4 h to remove any solvent, followed by heating at 150 °C for 4 h to promote the curing reaction.[39]

Preparation of composites

The epoxy resin (3.164 g) was mixed with the curing reagent (0.835 g) for 15 min and then degassed for 5 min using a conditioning mixer (AR-100, THINKY). The CNT/PBI was added (0.7 wt%) to the solution, stirred for 30 min with a high-shear mixing homogenizer (2500E, POLYTRON) at room temperature and further stirred at 70 °C for 3 h under vacuum. The blend cast

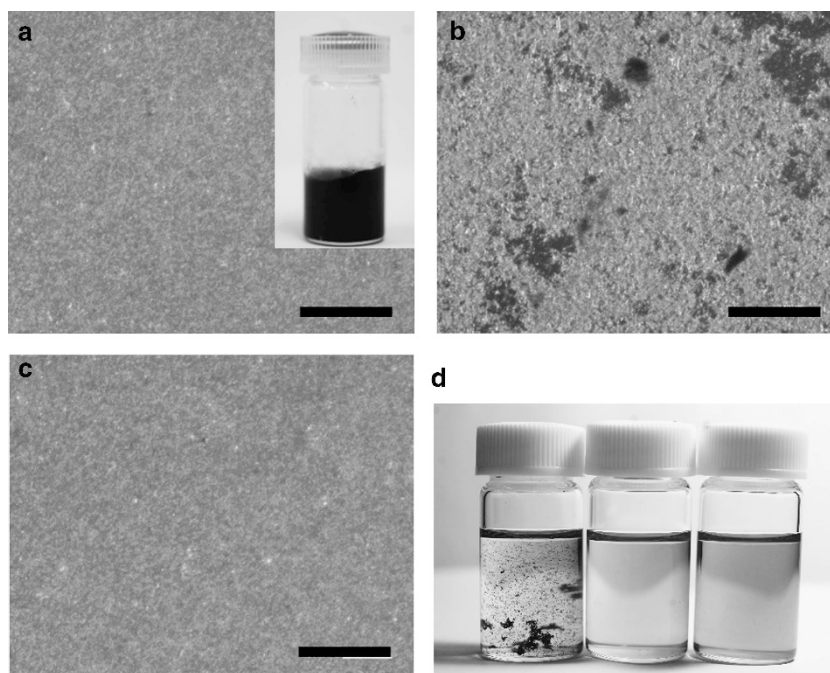Figure 2 (a–c) Optical microscopic images of the epoxy dispersion containing (a) CNT/PBI, (b) CNT and (c) oxCNT. The inset in a is a photo of the epoxy dispersion containing CNT/PBI. Scale bars represent 200 μm. (d) DMAc dispersions of CNTs (left), oxCNT (center) and CNT/PBI (right). CNT, carbon nanotube; DMAc, N,N-dimethylacetamide; PBI, polybenzimidazole. A full color version of this figure is available at Polymer Journal online.

on a Teflon mold ($60\,mm \times 30\,mm \times 10\,mm$) was cured at $100\,^{\circ}C$ for $2\,h$ followed by $150\,^{\circ}C$ for $4\,h$. The CNT-epoxy and oxCNT-epoxy composites were also prepared using a similar procedure.

RESULTS AND DISCUSSION

Model reactions

The key step in the present method is the chemical reaction between the PBI-coated CNTs and the epoxy resin. To confirm the ring opening reaction of an epoxy group by PBI upon heating, we carried out a model reaction between BI and glycidyl phenyl ether (Figure 1a). In the MS spectra of the product after mixing at $90\,^{\circ}C$ for $50\,h$, peaks were observed at $m/z = 461.24$ and 611.49, which correspond to a monoadduct (461.54) and diadduct (611.26), respectively (Figure 1b). These results indicate that the thermal reaction of the epoxy group with BI occurred. Furthermore, the reaction between PBI and the epoxy resin using a PBI/epoxy composite film prepared from the thermal treatment of the PBI/epoxy 100:20 (wt/wt) mixture at $80\,^{\circ}C$ for $4\,h$ and $150\,^{\circ}C$ for $4\,h$ was also carried out. The obtained

composite film was insoluble in DMAc, which is in contrast to the PBI film without the epoxy resin that is soluble in DMAc (Figure 1c). This result indicated that the reaction between PBI and the epoxy resin proceeded in the film,[39] and therefore, the cross-linking of PBI by the epoxy provided an insoluble material, as schematically illustrated in Figure 1d.

Preparation of composites

Next, the PBI-coated CNTs were incorporated into the epoxy resin. PBI-coated CNTs (CNT/PBI) were prepared according to a previously reported method.[27] An epoxy resin was mixed with CNT/PBI (0.7 wt%) at room temperature without using any solvents. As we previously reported,[26–29] the CNTs were homogeneously wrapped by PBI, the thickness of the PBI layer was $1 \sim 2\,nm$, and free PBI was not observed. The prepared CNT/PBI was efficiently dispersed in the epoxy resin because no visible aggregation was observed using optical microscope observations (Figure 2a). This result is in contrast to that
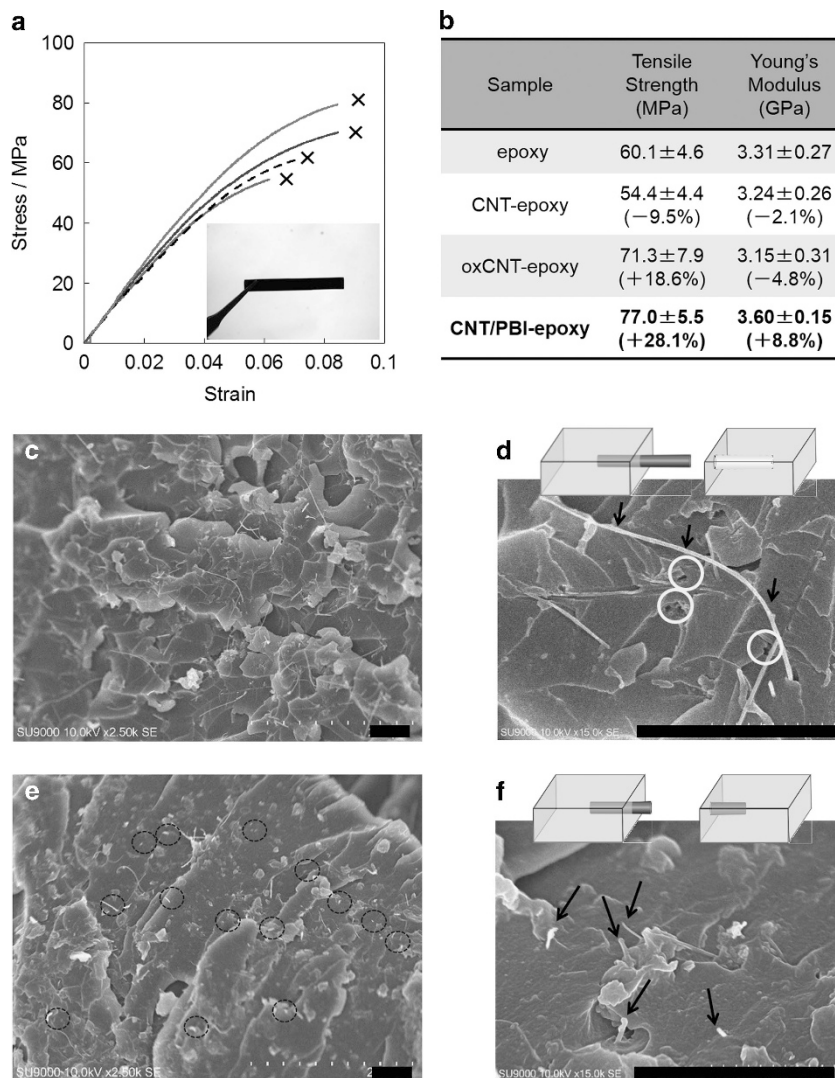

Figure 3 (**a**) Stress–strain curves of epoxy only (black line), CNT-epoxy (green line), oxCNT-epoxy (blue line) and CNT/PBI-epoxy (red line). (inset) Photo of the CNT/PBI-epoxy film. (**b**) Tensile strength and Young's modulus of epoxy only, CNT-epoxy, oxCNT-epoxy and CNT/PBI-epoxy. (**c–f**) SEM images of the fracture surface of oxCNT-epoxy (**c, d**) and CNT/PBI-epoxy (**e, f**) and at low (**c, e**) and high (**d, f**) magnification after the tensile tests. Black arrows and yellow circles indicated the CNTs and holes, respectively. The insets in **d** and **f** illustrate fractures of the composites. Scale bars represent $5\,\mu m$. CNT, carbon nanotube; PBI, polybenzimidazole; SEM, scanning electron microscopy. A full color version of this figure is available at *Polymer Journal* online.

Sample	Tensile Strength (MPa)	Young's Modulus (GPa)
epoxy	60.1±4.6	3.31±0.27
CNT-epoxy	54.4±4.4 (−9.5%)	3.24±0.26 (−2.1%)
oxCNT-epoxy	71.3±7.9 (+18.6%)	3.15±0.31 (−4.8%)
CNT/PBI-epoxy	**77.0±5.5 (+28.1%)**	**3.60±0.15 (+8.8%)**

observed for the sample using as-produced (non-functionalized) CNTs, which contained large aggregates (Figure 2b). We assume that good wettability between PBI and the epoxy resin would lead to effective dispersion of CNT/PBI in the epoxy resin. Because aggregation induces the force concentration and results in a severe decrease in strength,[40] we prepared oxidized CNTs (oxCNTs) as a control sample by plasma-assisted oxidation[41–43] and determined that oxCNTs exhibit no visible aggregation after mixing with the epoxy resin (0.7 wt%), as shown in Figure 2c. In addition, although the pristine CNTs aggregated in DMF, both oxCNTs and CNT/PBI exhibited good dispersion in the solvent, which indicates that the dispersibility of CNT/PBI is similar to that of oxCNTs (Figure 2d).

Homogeneous mixtures of the epoxy resin with 0.7 wt% of the CNT (CNT-epoxy), CNT/PBI (CNT-PBI-epoxy) and the oxCNT (oxCNT-epoxy)[44,45] were each cured in a Teflon mold to produce composite films (inset in Figure 3a). The mechanical properties of the obtained films were measured, and the representative stress–strain curves are shown in Figure 3a. It is important to note that CNT-epoxy (green line in Figure 3a) resulted in a large decrease of 9.5 and 2.1% in the tensile strength and Young's modulus, respectively, (Figure 3b) owing to aggregation of the CNTs in the epoxy matrices as shown in Figure 2b. This result confirms the negative impact of aggregation on the reinforcement. Importantly, CNT/PBI-epoxy exhibited a higher tensile strength (77.0 GPa) and Young's modulus (3.60 GPa) than those of oxCNT-epoxy (71.3 GPa and 3.15 GPa for tensile strength and Young's modulus, respectively). In addition, only CNT/PBI exhibited reinforcement in both the tensile strength (+28.1%) and Young's modulus (+8.8%) owing to the addition of CNTs (Figure 3b). Owing to the similar dispersion for both CNT/PBI and oxCNT in the epoxy matrices, the increased reinforcement in CNT/PBI-epoxy results from superior load transfer at the interface between CNT/PBI and the epoxy resin, which is most likely owing to the formation of covalent bonds between PBI and the epoxy matrix. In scanning electron microscopy measurements of the fracture surface after the tensile tests, long fiber structures and holes were observed for oxCNT-epoxy (Figures 3c and d), and short fibers were observed for CNT/PBI-epoxy (Figures 3e and f). As previously described,[5] the pulling of the long CNTs indicated insufficient load transfer between the CNTs and the matrix and that for the short CNTs, an effective load transfer is likely.[46] This result indicates that the PBI coated on the CNTs functioned as a glue to improve the load transfer at the epoxy/CNT interface.

CONCLUSIONS

In conclusion, we have developed a novel strategy for reinforcing an epoxy composite using PBI as a reactive glue for effectively introducing CNTs. The PBI coating on the surfaces of the CNTs enabled good dispersion of the tubes into the epoxy matrix. During thermal curing of the epoxy resin, the covalent bonds were formed between PBI and the epoxy group. Therefore, CNT/PBI exhibited an effective reinforcement of the epoxy resin, resulting in a higher tensile strength and Young's modulus (28.1 and 8.8%, respectively) than those of oxCNT (+18.6% and −4.8% for tensile strength and Young's modulus, respectively). Effective load transfer owing to the formation of covalent bonds in CNT/PBI-epoxy was also observed in the scanning electron microscopy measurements of the fracture surfaces, which possessed very short CNTs. This result is in contrast to that observed for oxCNT-epoxy, which contained long CNTs in the fracture surfaces.

The concept of polymer coating of CNTs with PBI is applicable not only to the reinforcement of composites containing CNTs but also to many other different carbon materials, such as CF, carbon black and graphene. Because PBI possesses very high thermal and chemical stability, the composites would be applicable for use under ultimate circumstances, which is an advantage of the current strategy.

CONFLICT OF INTEREST

The authors declare no conflict of interest.

1 Prusty, B. G., Sul, J. H. & Ray, T. Fatigue behaviour of short fibre composites (Nova Science Publishers, New York, NY, USA, 2011).
2 Jones, R. M. Mechanics of Composite Materials, 2nd edn (Taylor & Francis, Philadelphia, PA, USA, 1999)
3 Yu, M. F., Lourie, O., Dyer, M. J., Moloni, K., Kelly, T. F. & Ruoff, R. S. Strength and breaking mechanism of multiwalled carbon nanotubes under tensile load. Science 287, 637–640 (2000).
4 Song, Y. S. & Youn, J. R. Influence of dispersion states of carbon nanotubes on physical properties of epoxy nanocomposites. Carbon 43, 1378–1385 (2005).
5 Kingston, C., Zepp, R., Andrady, A., Boverhof, D., Fehir, R., Hawkins, D., Roberts, J., Sayre, P., Shelton, B., Sultan, Y., Vejins, V. & Wohlleben, W. Release characteristics of selected carbon nanotube polymer composites. Carbon 68, 33–57 (2014).
6 Andrews, R. & Weisenberger, M. C. Carbon nanotube polymer composites. Curr. Opin. Solid State Mater. Sci. 8, 31–37 (2004).
7 Baughman, R. H., Zakhidov, A. A. & de Heer, W. A. Carbon nanotubes-the route toward applications. Science 297, 787–792 (2002).
8 Breuer, O. & Sundararaj, U. Big returns from small fibers: a review of polymer/carbon nanotube composites. Polym. Compos. 25, 630–645 (2004).
9 Coleman, J. N., Khan, U., Blau, W. J. & Gun'ko, Y. K. Small but strong: a review of the mechanical properties of carbon nanotube-polymer composites. Carbon 44, 1624–1652 (2006).
10 Coleman, J. N., Khan, U. & Gun'ko, Y. K. Mechanical reinforcement of polymers using carbon nanotubes. Adv. Mater. 18, 689–706 (2006).
11 Harris, P. J. F. Carbon nanotube composites. Int. Mater. Rev. 49, 31–43 (2004).
12 Jiang, L., Tan, H., Wu, J., Huang, Y. & Hwang, K.-C. Continuum modeling of interfaces in polymer matrix composites reinforced by carbon nanotubes. Nano 2, 139–148 (2007).
13 Moniruzzaman, M. & Winey, K. I. Polymer nanocomposites containing carbon nanotubes. Macromolecules 39, 5194–5205 (2006).
14 Thostenson, E. T., Ren, Z. & Chou, T. W. Advances in the science and technology of carbon nanotubes and their composites: a review. Compos. Sci. Technol. 61, 1899–1912 (2001).
15 Wang, C., Guo, Z.-X., Fu, S., Wu, W. & Zhu, D. Polymers containing fullerene or carbon nanotube structures. Prog. Polym. Sci. 29, 1079–1141 (2004).
16 Xie, X.-L., Mai, Y.-W. & Zhou, X.-P. Dispersion and alignment of carbon nanotubes in polymer matrix: a review. Mater. Sci. Eng. R R49, 89–112 (2005).
17 Zhang, J. & Jiang, D. Interconnected multi-walled carbon nanotubes reinforced polymer-matrix composites. Compos. Sci. Technol. 71, 466–470 (2011).
18 Guo, P., Chen, X., Gao, X., Song, H. & Shen, H. Fabrication and mechanical properties of well-dispersed multiwalled carbon nanotubes/epoxy composites. Compos. Sci. Technol. 67, 3331–3337 (2007).
19 Ma, H., Zhao, L., Liu, J., Wang, J. & Xu, J. Functionalizing carbon nanotubes by grafting cyclotriphosphazene derivative to improve both mechanical strength and flame retardancy. Polym. Compos. 35, 2187–2193 (2014).
20 Wang, S., Liang, R., Wang, B. & Zhang, C. Load-transfer in functionalized carbon nanotubes/polymer composites. Chem. Phys. Lett. 457, 371–375 (2008).
21 Zhu, J., Kim, J., Peng, H., Margrave, J. L., Khabashesku, V. N. & Barrera, E. V. Improving the dispersion and integration of single-walled carbon nanotubes in epoxy composites through functionalization.. Nano Lett. 3, 1107–1113 (2003).
22 Wu, S.-Y., Yuen, S.-M., Ma, C.-C. M., Chiang, C.-L., Huang, Y.-L., Wu, H.-H., Teng, C.-C., Yang, C.-C. & Wei, M.-H. Preparation, morphology, and properties of silane-modified MWCNT/epoxy composites. J. Appl. Polym. Sci. 115, 3481–3488 (2010).
23 Gonzalez-Dominguez, J. M., Diez-Pascual, A. M., Anson-Casaos, A., Gomez-Fatou, M. A. & Martinez, M. T. Epoxy composites with covalently anchored amino-functionalized SWNTs: towards the tailoring of physical properties through targeted functionalization. J. Mater. Chem. 21, 14948–14958 (2011).
24 Wang, S. & Qiu, J. Modification of epoxy resins via m-chloroperbenzoic acid-epoxidized carbon nanotubes. J. Appl. Polym. Sci. 112, 3322–3326 (2009).

25 Yamamoto, G., Suk, J. W., An, J., Piner, R. D., Hashida, T., Takagi, T. & Ruoff, R. S. The influence of nanoscale defects on the fracture of multi-walled carbon nanotubes under tensile loading. *Diamond Relat. Mater.* **19**, 748–751 (2010).

26 Okamoto, M., Fujigaya, T. & Nakashima, N. Individual dissolution of single-walled carbon nanotubes (SWNTs) using polybenzimidazole (PBI) and high effective reinforcement of SWNTs/PBI composite films. *Adv. Funct. Mater.* **18**, 1776–1782 (2008).

27 Okamoto, M., Fujigaya, T. & Nakashima, N. Design of an assembly of poly(benzimidazole), carbon nanotubes, and Pt nanoparticles for a fuel-cell electrocatalyst with an ideal interfacial nanostructure. *Small* **5**, 735–740 (2009).

28 Fujigaya, T., Okamoto, M. & Nakashima, N. Design of an assembly of pyridine-containing polybenzimidazole, carbon nanotubes and Pt nanoparticles for a fuel cell electrocatalyst with a high electrochemically active surface area. *Carbon* **47**, 3227–3232 (2009).

29 Fujigaya, T. & Nakashima, N. Fuel cell electrocatalyst using polybenzimidazole-modified carbon nanotubes as support materials. *Adv. Mater.* **25**, 1666–1681 (2013).

30 Heise, M. S. & Martin, G. C. Curing mechanism and thermal properties of epoxy-imidazole systems. *Macromolecules* **22**, 99–104 (1989).

31 Fang, W., Jun, X., Jing-Wen, W. & Shu-Qin, L. A novel imidazole derivative curing agent for epoxy resin: synthesis, characterization, and cure kinetic. *J. Appl. Polym. Sci.* **107**, 223–227 (2008).

32 Ooi, S. K., Cook, W. D., Simon, G. P. & Such, C. H. DSC studies of the curing mechanisms and kinetics of DGEBA using imidazole curing agents. *Polymer* **41**, 3639–3649 (2000).

33 Ghaemy, M. & Sadjady, S. Kinetic analysis of curing behavior of diglycidyl ether of bisphenol A with imidazoles using differential scanning calorimetry techniques. *J. Appl. Polym. Sci.* **100**, 2634–2641 (2006).

34 Yan, Y., Cui, J., Zhao, S., Zhang, J., Liu, J. & Cheng, J. Interface molecular engineering of single-walled carbon nanotube/epoxy composites. *J. Mater. Chem.* **22**, 1928–1936 (2012).

35 Zhao, S., Song, Z., Cui, J., Li, C. & Yan, Y. Improving dispersion and integration of single-walled carbon nanotubes in epoxy composites by using a reactive noncovalent dispersant. *J. Polym. Sci. A Polym. Chem.* **50**, 4548–4556 (2012).

36 Fujigaya, T. & Nakashima, N. Non-covalent polymer wrapping of carbon nanotubes and the role of wrapped polymers as functional dispersants. *Sci. Technol. Adv. Mater.* **16**: Art. No. 024802 (2015).

37 Fu, L., Pan, M., Li, Y.-H., Wu, H.-B., Wang, H.-P., Yan, C., Li, K., Wei, S.-C., Wang, Z. & Su, C.-Y. A butterfly-like yellow luminescent Ir(III) complex and its application in highly efficient polymer light-emitting devices. *J. Mater. Chem.* **22**, 22496–22500 (2012).

38 Banfi, A., Benedini, F. & Sala, A. Synthesis of new imidazole derivatives as potential inhibitors of thromboxane synthetase. II. *J. Heterocycl. Chem.* **28**, 401–404 (1991).

39 Wang, S., Zhang, G., Han, M., Li, H., Zhang, Y., Ni, J., Ma, W., Li, M., Wang, J., Liu, Z., Zhang, L. & Na, H. Novel epoxy-based cross-linked polybenzimidazole for high temperature proton exchange membrane fuel cells. *Int. J. Hydrogen Energy* **36**, 8412–8421 (2011).

40 Ajayan, P. M. & Tour, J. M. Materials science: nanotube composites. *Nature* **447**, 1066–1068 (2007).

41 Felten, A., Bittencourt, C., Pireaux, J. J., Van Lier, G. & Charlier, J. C. Radio-frequency plasma functionalization of carbon nanotubes surface O2, NH3, and CF4 treatments. *J. Appl. Phys.* **98**, 074308 (2005).

42 Seo, M.-K., Park, S.-J. & Lee, S.-K. Influence of atmospheric plasma on physicochemical properties of vapor-grown graphite nanofibers. *J. Colloid Interface Sci.* **285**, 306–313 (2005).

43 Datsyuk, V., Kalyva, M., Papagelis, K., Parthenios, J., Tasis, D., Siokou, A., Kallitsis, I. & Galiotis, C. Chemical oxidation of multiwalled carbon nanotubes. *Carbon* **46**, 833–840 (2008).

44 Cui, L.-J., Geng, H.-Z., Wang, W.-Y., Chen, L.-T. & Gao, J. Functionalization of multi-wall carbon nanotubes to reduce the coefficient of the friction and improve the wear resistance of multi-wall carbon nanotube/epoxy composites. *Carbon* **54**, 277–282 (2013).

45 Gojny, F. H., Nastalczyk, J., Roslaniec, Z. & Schulte, K. Surface modified multi-walled carbon nanotubes in CNT/epoxy-composites. *Chem. Phys. Lett.* **370**, 820–824 (2003).

46 Li, S., Wang, F., Wang, Y., Wang, J., Ma, J. & Xiao, J. Effect of acid and TETA modification on mechanical properties of MWCNTs/epoxy composites. *J. Mater. Sci.* **43**, 2653–2658 (2008).